Malacological Applications of Scanning Electron Microscopy I. Introduction and Shell Surface Features

BY

ALAN SOLEM

Department of Zoology, Field Museum of Natural History
Roosevelt Road at Lake Shore Drive, Chicago, Illinois 60605

(Plates 58 to 60)

Observation and illustration of shell features in micromollusks have presented nearly insoluble problems to generations of malacologists. Using an optical microscope, details cannot be seen at very low magnifications, while at high magnification the depth of field is extremely shallow and there is not enough light available to distinguish finer structures. Photographic efforts generally are even less successful. The low resolving power of camera lenses, their very shallow depth of field, lighting problems, and the graininess of the film emulsion result either in minute images with little detail or large pictures with some areas obviously out of focus and details in other regions obscured by dark shadows. Various ingenious lighting techniques can reduce some of these difficulties (Blaker, 1961), but nothing can solve the optical depth of field limitations. Use of a "camera lucida" to prepare outline drawings of small shells or to establish proportions for an artist to make either a pen and ink or tone drawing has been a partially effective alternative. The Wild M-5 stereoscopic dissecting microscope with camera lucida, for example, is a superb instrument and very easy to use. Considerable time in reconstructing out of focus areas is required, the cost of illustration is high, and fine details are completely absent.

In the last three years, commercial versions of the scanning electron microscope have been installed in a number of universities and industrial laboratories. Although there is as yet little published work on mollusks resulting from use of this instrument, already it is evident that within a very few years the scanning electron microscope (hereafter SEM) will be the routine working tool for both examination and illustration of small mollusks. Its impact on pollen studies and entomology already has been dramatic. Even when renting SEM time at commercial rates, the cost of illustrations is competitive with good quality art work. Both the information content and quality of the SEM photographs are far superior to optical photographs or drawings.

In the past 18 months I have been able to spend about 25 hours studying shell sculpture and radulae with a Cambridge Mark I Stereoscan microscope at Alpha Research and Development, Inc. of Blue Island, Illinois. Mr. John A. Brown, electron microscopist, and his assistants have been of invaluable help in interpreting puzzling features. Equally important, their skill and efficiency in operation of the SEM has enabled completion of an amazing number of photographs and opened up whole new vistas for research. An equal debt is owed to the National Science Foundation who permitted illustration funds from NSF GB-6779 to be used in making the photographs reproduced here and to the administration of Field Museum for providing additional funds for exploratory studies. Mr. Fred Huysmans of the Field Museum photography department took infinite patience in coaxing maximum information from the polaroid negatives.

The present report is intended as an introduction to the capabilities of the SEM and its applicability to the study and illustration of shell surface features. A second report will cover data on radulae. Papers by Wise & Hay (1968a, 1968b), Taylor, Kennedy & Hall (1969), Erben, Flajs & Siehl (1968), and Wise (1969) have been concerned with cross-sectional structures of molluscan shells. Thompson & Hinton (1968) and Solem (1969) have published popular notes on shell sculpture studies. An extensive bibliography of scanning electron micrography is contained in the same volume as Wise (1969). Hay & Sandberg (1967) give an excellent introduction to the subject. Most of my own comments concerning technical specifications are paraphrased from these sources or from information provided by John Brown of Alpha Research.

OPTICAL VERSUS SEM VIEWING

Advantages of the SEM over optical equipment lie in a 50 to 500× increase in depth of field at a given magnification, 12½ to 100× increase in resolving power, a magnification range of 20 to 50 000× requiring clicks of a single dial, and the ability to rotate, tilt, and turn the specimen being examined while keeping it continuously in view. A comparison of the best quality stereoscopic dissecting microscope, compound light microscope, and SEM capabilities is given in Table I. This is modified from HAY & SANDBERG (1967, p. 410) with some additional data.

Optical systems have a depth of field that may be only one-twentieth the field of vision width, but the SEM has a depth of field that can reach five times the field of vision width. The significance of this in illustrating globular objects such as shells cannot be overemphasized. Using the lowest magnification (20×) of the Cambridge Mark IIa Stereoscan instrument at standard working distance, for example, any cylindrical shell whose length is less than 7 mm can be photographed in a single exposure and the image fills a 3½×3½ inch negative. Specimens of up to 12 mm in length can be photographed in two shots with a montage print producing one continuous image for reproduction. All portions of such a shell will be in focus. The lighting effect will approximate that of natural sunlight on a cloudy day. Details will be visible in all areas and proper contrast control will prevent heavy shadow effects. Heliciform shells of 5 mm diameter can be photographed in one shot. Even all parts of the apertural view will be completely in focus and details can be seen far inside the aperture. Montage photographs of 5 - 10 mm heliciform specimens would be possible with 3 to 4 exposures. Since the specimen position can be altered under fine control, after the first photograph is taken, tilting of a few degrees and taking a second photograph will yield a stereo pair. Standard photogrammetric equipment such as the Wild ST-4 Mirror Stereoscope with parallax bar will enable relative depth measurements of surface topography and three-dimensional viewing of the specimen.

At the lowest magnifications, the SEM can produce whole specimen illustrations of 5 to 7 mm shells. A magnification dial permits parfocal switching between 20, 50, 100, 300, 1 000, 3 000, 10 000, 30 000, and 50 000× in order to inspect structural details. Figures 3 to 11 present part of such a series. At each step the specimen can be moved and adjusted, changing the angle of view or shifting to a different area. It is visible at all times unless moved out of the scanning field by too enthusiastic spinning of controls! If "lost", returning to a lower magnification will relocate and enable retrieval of the strayed item.

SEM OPERATION

A series of electromagnetic lenses in a vacuum chamber focus a beam of electrons into an electron probe of 50 to

Table 1

Comparative Instrument Performance

	Stereoscopic Binocular Microscope	Compound Light Microscope	Scanning Electron Microscope
Resolution	20 000 Å	2 500 Å	200 Å
Field of view at:			
20 ×	12.5 mm circle 9.4 mm square	not normally used	5 × 5 mm
50 ×	4 mm circle 3 mm square	2.1 mm circle	2 × 2 mm
500 ×	—	0.21 mm circle	0.2 × 0.2 mm
5 000 ×	—	—	0.02 × 0.02 mm
50 000 ×	—	—	0.002 × 0.002 mm
Depth of field at:			
20 ×	0.5 mm	not normally used	+ 20 mm
50 ×	0.2 mm	0.02 mm	10 mm
500 ×	—	0.002 mm	1 mm
5 000 ×	—	—	0.1 mm
50 000 ×	—	—	0.01 mm

75Å diameter. When this beam hits a surface, a few electrons are reflected, but a much greater number of low energy secondary electrons are emitted from the surface. These electrons are caught by a detector, the signal amplified several thousand times, and displayed as a spot on a long persistence phosphor cathode ray tube. Image brightness is determined by the intensity of secondary electron emission, with a low emission rate producing a dim spot and a high emission rate producing a bright spot. Use of a sawtooth generator scans the focused electron beam across the specimen. By making a quick scan, it is possible to build and maintain a complete visual image on the long persistence phosphor cathode ray tube. It is this electronic image that one watches. Movements of the specimen produce a few seconds of distorted image until the previous scan spots fade and a new image builds up.

Producing a photograph requires use of a second cathode ray tube. In 100 seconds a single slow scan sweep is made onto a low persistence phosphor cathode ray tube. During this sweep the tube image is exposed to Polaroid Type 55 positive-negative film. After 20 seconds developing time, a Polaroid black and white print plus a negative are available for inspection. If brightness, contrast, or exposure was miscalculated, then a second picture can be taken immediately. About 5 minutes are required for each exposure, including control adjustments after magnification and specimen positioning have been selected. About 10 publishable exposures can be made per hour.

Since the image was scanned onto the cathode ray tube, attempts to enlarge a photograph more than 3 or 4× soon reveal the raster lines familiar to all TV watchers. Enlargement of the upper right hand corner in Figure 1 to full picture size (Figure 2) illustrates this problem. Huge enlargements can be made by "fuzzing" the enlarger focus, but this results in significant detail loss.

SPECIMEN PREPARATION AND SIZE LIMITS

For dissipation of any electron charge that builds up on non-conductive surfaces, a conductive surface is desirable. Metallic substances can be examined directly, but biological specimens and fossils either must be given a conductive coating or else have the electron beam reduced to between 1 to 3 kV. Great loss of resolution in the image results from the latter option. Gold, palladium, aluminum, platinum and carbon are commonly used coating materials. For effective viewing, a clean surface is essential.

The specimens illustrated in this report were first cleaned of most dirt and incrustations by soaking overnight in water and then immersion for a few seconds into a water-filled tank of an ultrasonic cleaner. They were attached to a SEM stub with ordinary rubber cement and then placed in a vacuum evaporator. After pressure had been reduced to 10^{-4} torr, a 200 - 300 Å layer of gold or aluminum was vaporized electrically in a tungsten filament while the specimen was rotated slowly beneath the filament. This allowed relatively even coating of complex surface topography. The gilded stub was taken from the vacuum evaporator and transferred into the SEM specimen chamber. After pumping the electron column and chamber down to 10^{-5} torr, study was undertaken.

Special equipment permits insertion of specimens up to 36 mm in size, but movements are greatly restricted and there is no increase in the field of vision. A specimen 12 mm square and 3 mm high can be handled with no restrictions on adjustments.

MATERIALS

Figures 1 and 2 are of a Moorea, Society Island species formerly known as *"Charopa" modicella* (Férussac,

Explanation of Plate 58

"Charopa" modicella (Férussac, 1840)

Figures 1, 2: Faatoai Valley, Moorea, Society Islands. Bernice P. Bishop Museum number 150377. Figure 1: diagonal view onto apex and early postnuclear whorls at 335 × magnification. Figure 2: enlargement of upper right area from negative of Figure 1 to demonstrate presence of raster lines.

Ptychodon microundulata (Suter, 1890)

Figures 3 - 6: Turanganui River, Haurangi Range, Wellington, New Zealand. Dominion Museum, Wellington. Figure 3: General view of shell at 110 ×. Figure 4: Suture between nuclear and postnuclear region at 1 100 × showing apical (upper left) and post-apical (lower right) sculpture types. Surface debris on right side can be used to locate area photographed slightly above and to the left of center in Figure 3. Figure 5: Sutural area at end of nuclear whorls, 1 100 ×, showing tentative start of microradial sculpture and channeled suture. Photograph taken at 1⅝ whorl mark and showing post-apical sculpture at the end of the first complete postnuclear whorl. Figure 6: Detail of early apical sculpture at 3 350 × showing irregularly folded periostracum between two radial ribs. Folds can be matched with upper left portion of Figure 4 to establish size change.

Figure 1

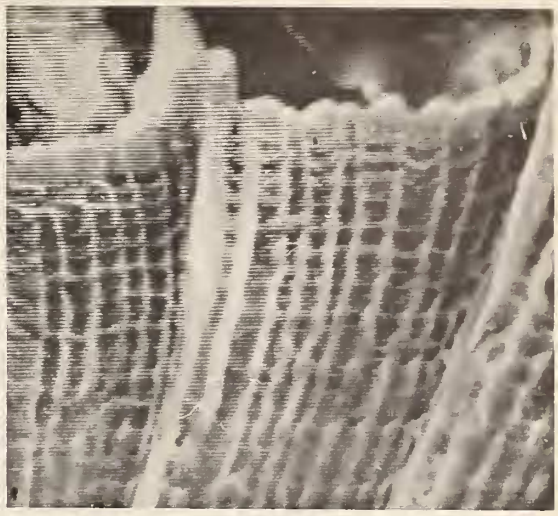

Figure 2

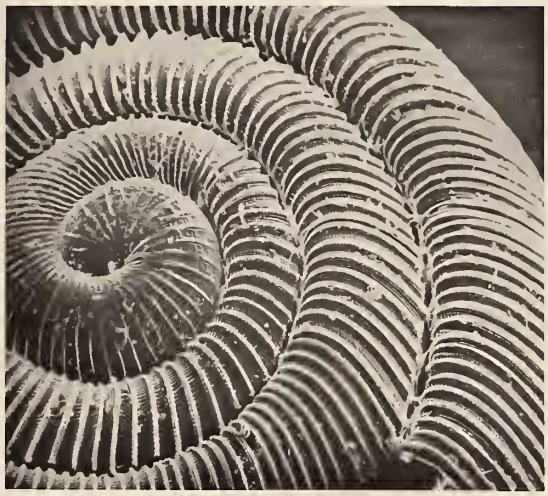

Figure 3

Figure 4

Figure 5

Figure 6

1840). It is an endodontid land snail belonging to the subfamily Charopinae, but is classified in a currently undescribed genus. The specimen is from Faatoai Valley and is Bernice P. Bishop Museum number 150377. Remaining figures are of the New Zealand endodontid *Ptychodon microundulata* (SUTER, 1890). Specimens were collected by A. C. O'Connor in June 1949 from the Turanganui River, Haurangi Range, Wellington and preserved as dry specimens at the Dominion Museum, Wellington. I am deeply indebted to the authorities of the Bishop Museum and Dominion Museum for permission to study this material.

RESULTS

Dissections of Pacific Island endodontid land snails had revealed anatomically quite distinctive subfamilies whose shell sculpture appeared to be virtually identical under optical microscope examination. Initial use of the SEM was in search of conchological features that would serve as subfamily or generic identification criteria. Expansion of this work into studies of functional aspects of shell sculpture and investigation of endodontid shells from other areas soon followed.

The Moorean specimen is tilted at about a 45° angle from a horizontal view. Figure 1 shows the apex and part of the first two postnuclear whorls in a shell measuring 3.25 mm in diameter with $4\frac{1}{4}$ whorls. Actual width of the first nuclear whorl, which is not completely shown in Figure 1, is about 0.38 mm. Both apical and postnuclear sculpture are typical for the Pacific Island Charopinae.

Ptychodon microundulata has a relatively complex and highly photogenic surface sculpture (Figures 3 to 11). All these photographs involve portions of a juvenile shell measuring 1.38 mm in diameter with $3\frac{3}{4}+$ whorls. Photographs of the parietal lamella (Figures 12 - 15) were taken from a slightly larger individual by breaking away the palatal wall so that a direct view could be obtained of the entire lamella. Optical examination at 100× had shown that the juvenile showed essentially no worn spots on the apex and postnuclear whorls. More information could be obtained from this specimen than from larger examples with obvious surface wear. Adult size for this species is 1.71 - 1.97 mm, $\overline{X}$ is 1.86 mm, S. E. M. is 0.024 mm with 10 specimens measured.

Figures 4 - 6 and 8 - 10 were taken during one visit to Alpha Research. Figures 3 and 7 were taken about two months later. Despite the specimen having been kept in a closed snap-lock plastic box, the concentration of particulate matter in Chicago air is obvious. More than half of this debris accumulated after the initial study.

Figure 3 at 110× indicates essentially what can be seen under optical examination, although only a small part of the shell would be in focus at any one time. Major shell sculpture consists of prominent radial ribs on both the apex (first $1\frac{5}{8}$ whorls) and postnuclear whorls. The radial ribs are more widely spaced on the early apex, become much more crowded on the last portion and then change in appearance at the start of postnuclear growth. While the presence of some kind of microsculpture between the radial ribs can be seen, its frequency and nature cannot be determined.

Although the texture of the interstices between the apical radial ribs looks different from the texture between the postnuclear radial ribs, no information is retrievable at 110×. Under optical examination, data gathering would stop. By switching the SEM to 1 100× and focusing on a suture between the first apical whorl and first postnuclear whorl (Figure 4), both microsculptures are displayed. The postnuclear portion (right and lower half) has a series of complex microradial riblets with enlarged "beads" that are arranged in spiral rows. Apical sculpture consists of irregular wrinkles and ridges with a "glassy" or "greasy" surface appearance. At 3 350× (Figure 6) this apical sculpture is confirmed as consisting of a smooth film (= periostracum) that is irregularly folded. Rotation of the specimen to the point of demarcation between apical and postnuclear whorls (Figure 5) and examination at 1 100× shows that tentative formation of the postnuclear micro-radial ridges begins a short distance before the end of the periostracal film. Regular production of the micro-radial ridges starts at the end of this folded film and coincides with the increase in rib spacing noticeable in the early postnuclear section of Figure 3.

Several other New Zealand endodontids and the Indonesian-Pacific Island *Discocharopa* have the same type of apical periostracum. An essentially equivalent type is seen in several European taxa that were photographed in cooperation with Dr. Gittenberger of Leiden. Interpretation of this structure is somewhat difficult. In physical characteristics, John A. Brown of Alpha Research informs me, this is the same pattern seen in many dried paint or varnish films at equivalent magnifications. With this knowledge, a hypothesis of origin can be suggested. Both the periostracum and calcified layer of the apical whorls are formed during a late embryonic stage. This takes place in liquid and the embryonic shell with firm calcification can be removed from unhatched eggs. Thus solidification of the calcium layer may occur while the periostracum is still bathed in liquid. If hardening of the periostracal layer was delayed until after hatching, then air drying of the periostracal film could result in the irregular folding

seen in the apical film. Differential frictional adherence of the film at the start of drying would result in the development of "tension folds" as it settled or shrank into position on top of the calcium layer. Possibly the initial movement of the snail from the ruptured egg shell or brushes against minute particles in the environment could shift or distort the wet and pliable film, thus producing the irregularities. Even rotational movements of the embryo within the egg capsule might be enough to produce the distortions. Determination of what is the time relationship between end of the apical sculpture and hatching will require study of young that were preserved minutes after hatching. While logic would suggest that hatching would coincide with the start of postnuclear sculpture formation, it is quite possible that it may precede hatching for a few ridges during the period when the embryo is actively moving but has not yet broken through the egg shell. This could be determined very easily with the SEM through study of pre-hatched, hatching, and recently hatched shells.

Returning to the postnuclear sculpture, at 335× (Figure 7) it is seen to consist of high major ribs that stop on the suture edge. From 3 to 7 micro-radial riblets lie in the trough between each pair of major ribs on the early sections. They also are present on both the sides and tops of the major ribs. Major ribs are $\frac{1}{3}$ to $\frac{1}{5}$ as wide as the interval between each pair and the spacing varies slightly from rib to rib. There are fewer micro-riblets between crowded than between widely spaced ribs. This leads to the conclusion that depositional timing of the micro-riblets and major ribs is independent. That is, production of a major rib is not started after "x" number of micro-riblets, but that control of these two sculptures is separate. Data on this aspect will be presented elsewhere. Optical examination of the shell had permitted counting the major ribs on the body whorl with an accuracy of ± 1. Knowing that the shell diameter was 1.38 mm, simple multiplication by π produced the shell circumference[1] of 4.34 mm. Division of the 124 ribs on the body whorl by the circumference in mm established there are an average of 28.6 major ribs per mm on the body whorl periphery.

By shifting to the body whorl periphery about $\frac{1}{4}$ whorl behind the aperture (Figures 8 to 11), it was possible to examine structural details of the postnuclear microsculpture. The basic orientation is looking down onto the body whorl top and curvature of the periphery with a slight angling towards the aperture. Whenever repetitive surface sculpture is present, viewing around a curve permits simultaneous inspection of the sculpture elements from various angles. This greatly aids interpretation and allows mental stereoscopic reconstruction of complex topography. In Figure 8 the magnification of 1 100× shows about 0.15 mm of body whorl periphery. Each major rib is seen to have a single, high, posteriorly recurved, slightly sinuated lamellar extension. Inspection at 3 350× in Figure 9 shows that this structure arises from the top of a microradial and that its surface shows traces of very irregular grooving. As the snail moves through leaf litter, this lamellar extension would brush against fine particles in the environment. Minute grains of rock and soil would rub against this reflected edge. As the snail moved forward, sharp edges on the miniature boulders would score or abrade the surface, producing the irregular grooves seen on its outer edge. This lamellar extension is not present during the first postnuclear whorl (Figures 3 to 5) and only weakly developed on the second postnuclear whorl (Figure 7). Most major ribs show partial evidence of minor extensions on the microradials just before and just after the major extension (Figures 8 to 10). An under-

[1] Although the actual measurement should have been one volution of the logarithmic growth curve to establish periphery length, this simple calculation is an adequate approximation. Rib counts are the same at the suture and periphery of a whorl although the linear distance is not the same. Bias is essentially the same for every specimen and is not considered significant.

Explanation of Plate 59

Ptychodon microundulata (Suter, 1890)

Figures 7 - 11: Turanganui River, Haurangi Range, Wellington, New Zealand. Same specimen used in Figures 3 - 6. Figure 7: Early apical and two whorls of post-apical sculpture at 335 ×. Note suture and "beaded" appearance of microradials except at curve into suture. Figure 8: Periphery of body whorl, one-quarter whorl behind aperture, at 1 100 ×. Note change in appearance of microradials as the curvature increases. Figure 9: Peripheral view between two major ribs at 3 350 × showing change in microradial buttress form and structure of microsculpture. Figure 10: Detail of microsculpture on periphery at 11 100 ×. Note change in buttress height and shape on ascending side of major ridge at right margin of photograph. Figure 11: Two "beads" on a microradial ridge at 33 500 × showing the ascending buttress structure (apical direction to left of figure, apertural direction to right). Figures 9 to 11 are enlarged details from the area shown in Figure 8.